Interface Debonding Prediction Technique for Tensile Loaded AA6061/Zirconium Oxide Nanoparticulate MMC

[1]P. M. Jebaraj and A. Chennakesava Reddy[2]

[1]Professor, Department of Mechanical Engineering, Dr. A. I.T, Bangalore, India
[2]Assistant Professor, Department of Mechanical Engineering, MJ College of Engineering and Technology, Hyderabad, India
dr_acreddy@yahoo.com

Abstract: A diamond array unit cell/2-D octahedron particulate RVE models were employed to evaluate interfacial debonding using cohesive zone analysis. The particulate metal matrix composites are zirconium oxide/AA6061 alloy at volume fractions of 10%, 20% and 30% boron nitride. Interface debonding was observed in all the composites at angle of 72^{o} from axis of loading.

Keywords: AA6061 alloy, zirconium oxide, octahedron particulate, RVE model, finite element analysis, interface debonding.

1. INTRODUCTION

Metal matrix composite (MMC) materials are superior to conventional monolithic materials for a number of reasons, noteworthy amongst these being their mechanical properties. The mechanism of failure at the microscale is dominated by factors such as the cohesive strength of the interface, and the strength and reliability of the particle and matrix phase. The interface between the reinforcement and matrix plays a crucial role in changing the property of composite material. In many cases the properties of MMC can be drastically altered by the nature of the interface, making it necessary to understand the characteristics of the interface. A number of different approaches have been considered for modeling the interface, among which the cohesive zone models are widely used to model delamination and debonding in composite materials [1-14].

The present study is on the interface debonding between AA6061 alloy and zirconium oxide nanoparticle. Representative volume elements (RVEs) models were taken from the periodic 2-D octahedron particulates in a diamond array distribution (figure 1).

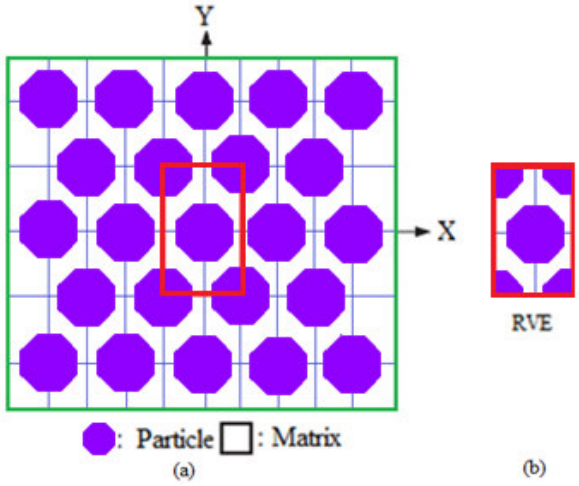

Figure 1: The RVE model.

2. MATERIALS AND METHODS

The computational domain considered in the current research is comprised of AA6061 alloy matrix material with an embedded 2-D octahedron zirconium oxide inclusion. The volume fractions of zirconium oxide were 10%, 20%, and 30%. In the model periodic boundary conditions were used in the x and y directions. Initially, both AA6061 and zirconium oxide were kept in contact along the interface in the x–y plane with zero separation distance. The simulation domain is divided into three regions: zirconium oxide nanoparticle, interface and AA6061 alloy matrix. PLANE183 element was used for the matrix and the

nanoparticulates. The cohesive zone can be incorporated in the continuum formulation by applying the cohesive tractions as boundary conditions. The cohesive element is implemented as a linear element with four nodes. Initially, the interface between the matrix material and the inclusion is assumed to be perfectly bonded, that is, continuity of traction and displacement is assumed along the interface. The finite element analysis was carried out for the single inclusion model undergoing a tensile load. The elastic material properties are given by E_m = 68.90 GPa, E_p = 250 GPa, ν_m = 0.33 and ν_p = 0.32.

Shear-log model is based on the assumption that all of the load transfer from matrix to particulate occurs via shear stresses acting on the particulate interface between the two constituents. The rate of change of the stress in the particulate to the interfacial shear stress at that point and the particulate radius, 'r' is given by:

$$\frac{d\sigma_p}{dx} = -\frac{2\tau_i}{r} \quad (1)$$

which may be regarded as the basic shear lag relationship.

The stress distribution in the particulate is determined by relating shear strains in the matrix around the particulate to the macroscopic strain of the composite. Some mathematical manipulation leads to a solution for the distribution of stress at a distance 'x' from the mid-point of the particulate which involves hyperbolic trig functions:

$$\sigma_p = E_p\varepsilon_c[1 - cosh(nx/r)sech(ns)] \quad (2)$$

where ε_c is the composite strain, s is the particulate aspect ratio (length/diameter) and n is a dimensionless constant given by:

$$n = \left[\frac{2E_m}{E_p(1+\nu_m)ln(1+\nu_p)}\right]^{1/2} \quad (3)$$

in which ν_m is the Poisson ratio of the matrix. The variation of interfacial shear stress along the particulate length is derived, according to Equation (1), by differentiating this equation, to give:

$$\tau_i = \frac{n\varepsilon_c}{2} E_p sinh\left(\frac{nx}{r}\right) sech(ns) \quad (4)$$

The equation for the stress in the particulate, together with the assumption of a average tensile strain in the matrix equal to that imposed on the composite, can be used to evaluate the composite stiffness. This leads to:

$$\sigma_c = \varepsilon_c\left[v_p E_p\left(1 - \frac{tanh(ns)}{ns}\right) + (1 - v_p)E_m\right] \quad (5)$$

The expression in square brackets is the composite stiffness. The stiffness is a function of particulate aspect ratio, particulate/matrix stiffness ratio and particulate volume fraction.

If the particle deforms in an elastic manner (according to Hooke's law) then,

$$\tau = \frac{n}{2}\sigma_p \quad (6)$$

If interfacial debonding/yielding is considered to occur when the interfacial shear stress reaches its shear strength

$$\tau = \tau_{max} \quad (7)$$

For particle/matrix interfacial fracture can be established whereby,

$$\tau_{max} < \frac{n\sigma_p}{2} \quad (8)$$

This approach suggests that the outcome of a matrix crack impinging on an embedded particle depends on the balance between the particle strength and the shear strength of the interface. For plane strain conditions, the macro stress- macro strain relation is as follows:

$$\begin{Bmatrix}\overline{\sigma_x}\\ \overline{\sigma_y}\\ \overline{\tau_{xy}}\end{Bmatrix} = \begin{bmatrix}\overline{C_{11}} & \overline{C_{12}} & 0\\ \overline{C_{21}} & \overline{C_{22}} & 0\\ 0 & 0 & \overline{C_{33}}\end{bmatrix} \times \begin{Bmatrix}\overline{\varepsilon_x}\\ \overline{\varepsilon_y}\\ \overline{\gamma_{xy}}\end{Bmatrix} \quad (9)$$

The interfacial tractions can be obtained by transforming the micro stresses at the interface as given in Eq. (3):

$$t = \begin{Bmatrix}t_z\\ t_n\\ t_t\end{Bmatrix} = T\sigma \quad (10)$$

where, $T = \begin{bmatrix}0 & 0 & 0\\ cos^2\theta & sin^2\theta & 2sin\theta cos\theta\\ -sin\theta cos\theta & sin\theta cos\theta & cos^2\theta - sin^2\theta\end{bmatrix}$

3. RESULTS AND DISCUSSION

The tensile and compression moduli increased with volume fraction of ZrO_2 as shown figure 2a. The shear modulus increased constant with increase in the volume fraction of ZrO_2 up to 20% Vp in the composites (figure 2b), while it was lower for 30%Vp of ZrO_2 than that of 10% and 20%Vp of ZrO_2. The major Poisson's ratio decreased with volume fraction of ZrO_2. The

stiffness mismatch between ZrO_2 nanoparticulate and AA6061 alloy matrix is 181 GPa. The condition $\tau_{max} < n\sigma_p/2$ is satisfied for the prevalence of interface debonding in the composites including 10%, 20% and 30% ZrO_2 (figure 3). The strain energy density developed in the composites is shown in figures 4 and 5. For the shearing of interface between ZrO_2 inclusion and AA6061 alloy matrix, the strain energy density at the interface was higher than that in ZrO_2 particle and AA6061 alloy matrix.

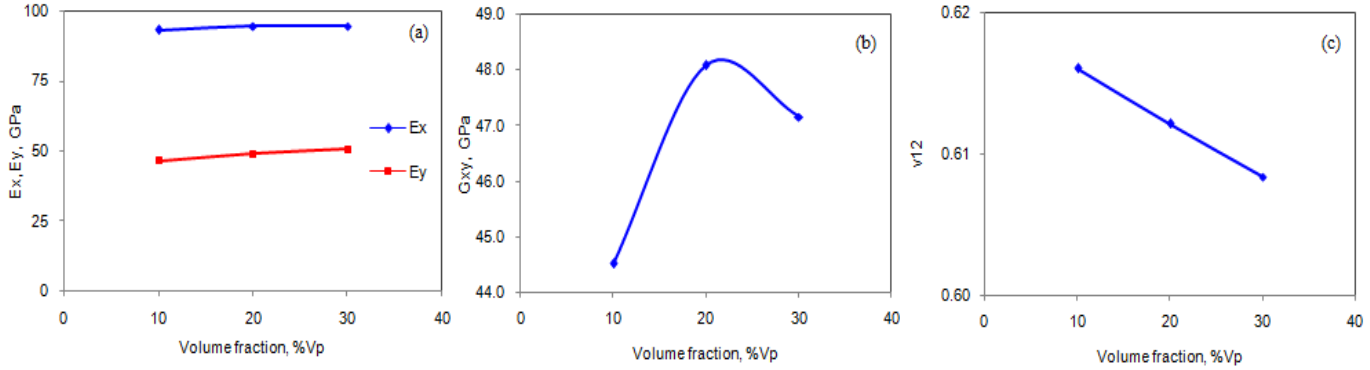

Figure 2: Effect of volume fraction on effective material properties.

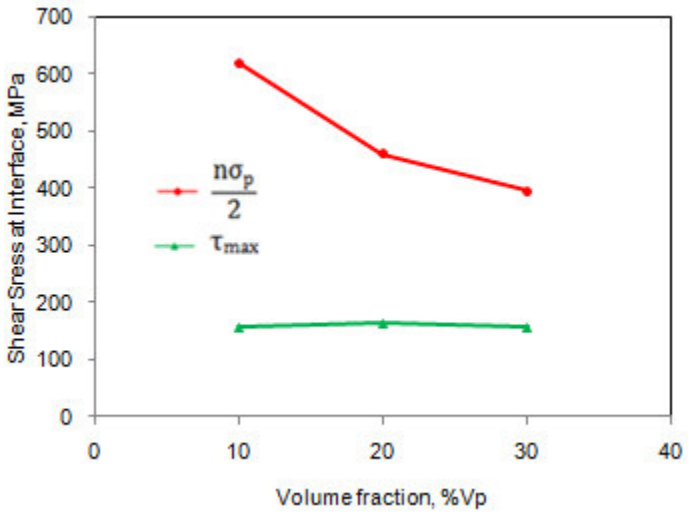

Figure 3: Fracture criteria of interface debonding.

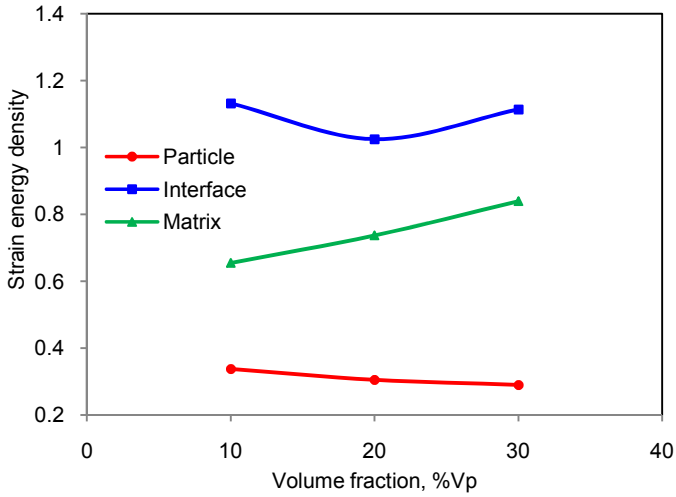

Figure 4: Effect of volume fraction on strain energy density.

The normal and tangential tractions are plotted in figure 6. As these traction stresses were calculated locally near the interface. The normal traction in the region of interface between ZrO_2 nanoparticulate and AA6061 alloy matrix was high in the direction (0^o) of tensile loading while it decreased with increase of angle along the interface. The maximum allowable normal and tangential separation of the cohesive element corresponds to the separation distance at which the traction decreases to near zero value. The separation took place at 72^o from the axis of loading for the octahedron nanoparticulate in the matrix of AA6061 alloy. The strain energy density at point of separation was 0.427 for the composites having 30% ZrO_2.

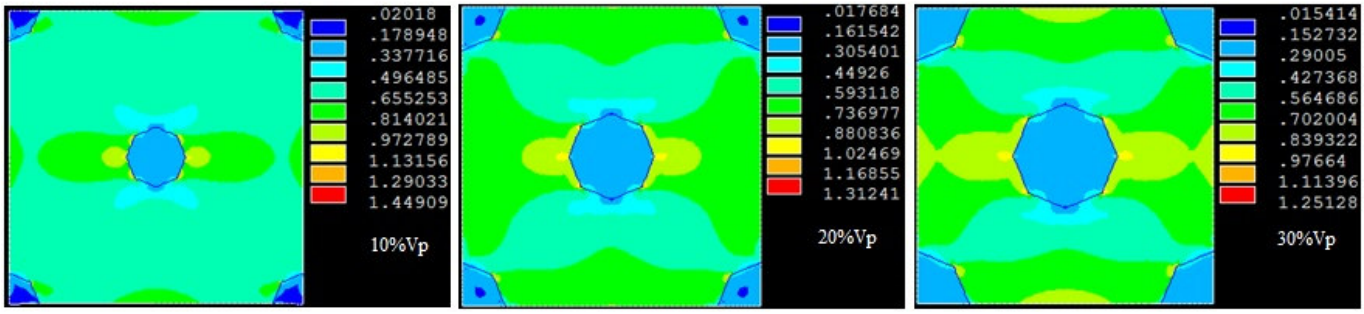

Figure 5: FEA results of strain energy densities.

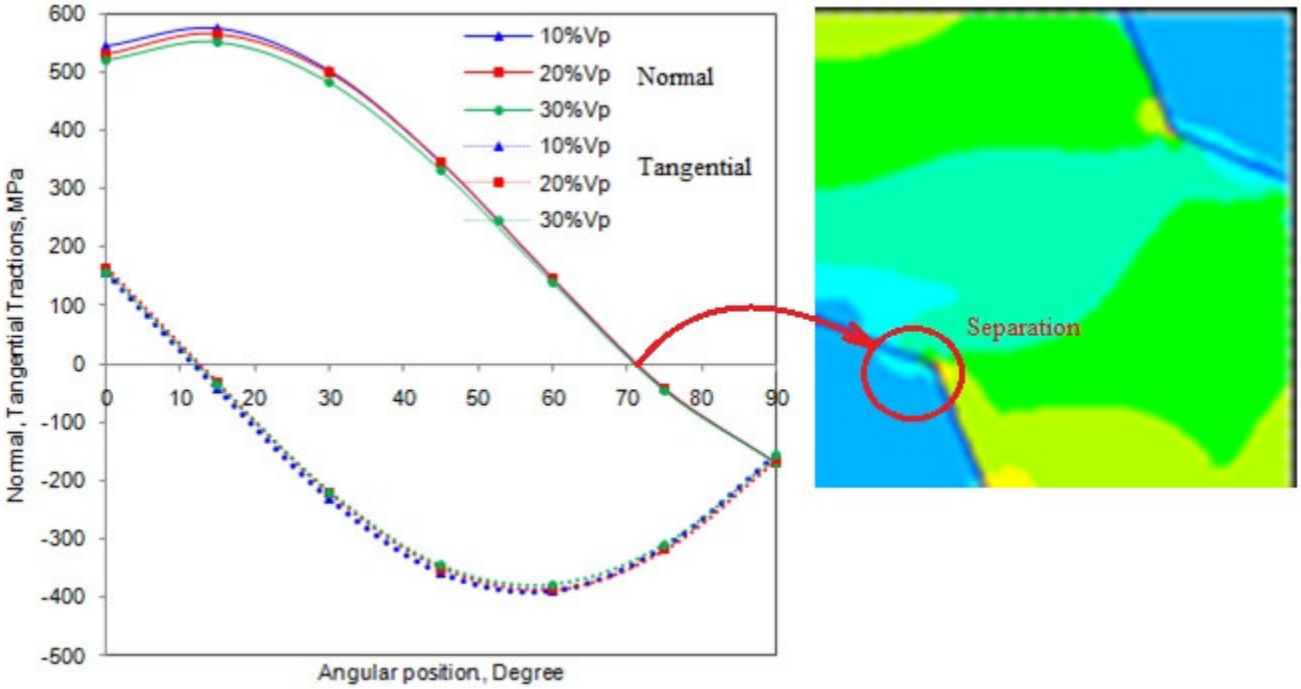

Figure 6: Normal and tangential: (a) tractions and (b) displacements.

4. CONCLUSION

The interface debonding occurred in the composites containing 10%, 20% and 30% volume fractions ZrO_2. As these stresses were calculated locally near the interface they therefore relate to the traction in the traction–separation law. The maximum strain densities at which the traction decreases to near zero value were 0.497, 0.449 and 0.427, respectively, for 10%, 20% and 30% ZrO_2 inclusions in AA6061 alloy matrix.

REFERENCES

1. A. Chennakesava Reddy, Assessment of Debonding and Particulate Fracture Occurrences in Circular Silicon Nitride Particulate/AA5050 Alloy Metal Matrix Composites , National Conference on Materials and Manufacturing Processes, Hyderabad, India, 27-28 February1998, pp.104-109.

2. B. Kotiveera Chari and A. Chennakesava Reddy, Numerical Simulation of Particulate Fracture in Round Silicon Nitride Particulate/AA6061 Alloy Metal Matrix Composites, National Conference on Materials and Manufacturing Processes, Hyderabad, India, 27-28 February 1998, pp. 110-114.
3. H. B. Niranjan and A. Chennakesava Reddy, Effect of Elastic Moduli Mismatch on Particulate Fracture in AA7020/Silicon Nitride Particulate Metal Matrix Composites , National Conference on Materials and Manufacturing Processes, Hyderabad, India, 27-28 February, 1998, pp. 115-118,
4. P. Martin Jebaraj and A. Chennakesava Reddy, Cohesive Zone Modelling for Interface Debonding in AA8090/Silicon Nitride Nanoparticulate Metal Matrix Composites, National Conference on Materials and Manufacturing Processes, Hyderabad, India, 27-28 February 1998, pp. 119-122.
5. P. Martin Jebaraj and A. Chennakesava Reddy, Plane Strain Finite Element Modeling for Interface Debonding in AA1100/Silicon Oxide Nanoparticulate Metal Matrix Composites, National Conference on Materials and Manufacturing Processes, Hyderabad, India, 27-28 February 1998, pp. 123-126.
6. A. Chennakesava Reddy, Local Stress Differential for Particulate Fracture in AA2024/Titanium Carbide Nanoparticulate Metal Matrix Composites, National Conference on Materials and Manufacturing Processes, Hyderabad, India, 27-28 February 1998, pp. 127-131.
7. B. Kotiveera Chari and A. Chennakesava Reddy, Interface Debonding and Particulate Facture based on Strain Energy Density in AA3003/MgO Nanoparticulate Metal Matrix Composites, National Conference on Materials and Manufacturing Processes, Hyderabad, India, 27-28 February 1998, pp. 132-136.
8. H. B. Niranjan and A. Chennakesava Reddy, Numerical and Analytical Prediction of Interface Debonding in AA4015/Boron Nitride Nanoparticulate Metal Matrix Composites , National Conference on Materials and Manufacturing Processes, Hyderabad, India, 27-28 February 1998, pp. 137-140.
9. S. Sundara Rajan and A. Chennakesava Reddy, Effect of Particulate Volume Fraction on Particulate Cracking in AA5050/Zirconium Oxide Nanoparticulate Metal Matrix Composites , National Conference on Materials and Manufacturing Processes, Hyderabad, India, 27-28 February 1998, pp. 156-159.
10. S. Sundara Rajan and A. Chennakesava Reddy, Cohesive Zone Analysis for Interface Debonding in AA6061/Titanium Nitride Nanoparticulate Metal Matrix Composites , National Conference on Materials and Manufacturing Processes, Hyderabad, India, 27-28 February 1998, pp. 160-164.
11. A. Chennakesava Reddy, Effect of Particle Loading on Microealstic Behavior and interfacial Tractions of Boron Carbide/AA4015 Alloy Metal Matrix Composites, 1st International Conference on Composite Materials and Characterization, Bangalore, 14-15 march 1997, pp. 176-179.7
12. A. Chennakesava Reddy, Reckoning of Micro-stresses and interfacial Tractions in Titanium Boride/AA2024 Alloy Metal Matrix Composites, 1st International Conference on Composite Materials and Characterization, Bangalore, 14-15 march 1997, pp. 195-197.
13. A. Chennakesava Reddy, Interfacial Debonding Analysis in Terms of Interfacial Tractions for Titanium Boride/AA3003 Alloy Metal Matrix Composites, 1st National Conference on Modern Materials and Manufacturing , Pune, India, 19-20 December 1997, pp. 124-127.
14. A. Chennakesava Reddy, Evaluation of Debonding and Dislocation Occurrences in Rhombus Silicon Nitride Particulate/AA4015 Alloy Metal Matrix Composites, 1st National Conference on Modern Materials and Manufacturing , Pune, India, 19-20 December 1997, pp. 278-282.